ChemPubSoc Europe

DOI: 10.1002/cssc.201601171

CHEMSUSCHEM Full Papers

Chemical and Photochemical Water Oxidation Mediated by an Efficient Single-Site Ruthenium Catalyst

Ahmed F. Abdel-Magied,[a] Andrey Shatskiy,[a] Rong-Zhen Liao,[b] Tanja M. Laine,[a] Wael A. A. Arafa,[a, c] Per E. M. Siegbahn,[a] Markus D. Kärkäs,*[a] Björn Åkermark,*[a] and Eric V. Johnston*[a]

Water oxidation is a fundamental step in artificial photosynthesis for solar fuels production. In this study, we report a single-site Ru-based water oxidation catalyst, housing a dicarboxylate-benzimidazole ligand, that mediates both chemical and light-driven oxidation of water efficiently under neutral conditions. The importance of the incorporation of the negatively charged ligand framework is manifested in the low redox potentials of the developed complex, which allows water oxidation to be driven by the mild one-electron oxidant $[Ru(bpy)_3]^{3+}$ (bpy = 2,2′-bipyridine). Furthermore, combined experimental and DFT studies provide insight into the mechanistic details of the catalytic cycle.

Introduction

In Nature, green plants, cyanobacteria, and algae utilize solar energy to split water and fix CO_2 for the production of biomass. In this process, photosynthesis, water is oxidized catalytically to O_2 [Eq. (1)] by the oxygen-evolving complex (OEC), which comprises an asymmetric Mn_4CaO_5 cluster.[1] The splitting of water into O_2 and H_2 is an attractive approach for the production of clean and sustainable chemical energy. For this to be realized, mimicking or even surpassing the efficiency of the OEC is a critical issue for the development of commercially viable synthetic water oxidation catalysts (WOCs). Considerable progress has been made during recent years in the development of molecular catalysts for water oxidation based on transition metals, such as Mn,[2] Co,[3] Fe,[4] Cu,[5] Ir,[6] and Ru.[7]

$$2\,H_2O \rightarrow O_2 + 4\,H^+ + 4\,e^- \qquad (1)$$

Among the developed WOCs, single-site Ru-based catalysts are among the most efficient for the oxidation of water as they offer synthetic flexibility, and facilitate mechanistic studies. The majority of these studies have employed $(NH_4)_2[Ce^{IV}(NO_3)_6]$ (ceric ammonium nitrate; CAN) as a terminal oxidant; however, other chemical oxidants have also been explored, such as $[Ru(bpy)_3]^{3+}$ (bpy = 2,2′-bipyridine),[3a,7g] OCl^-,[8] and HSO_5^-.[9]

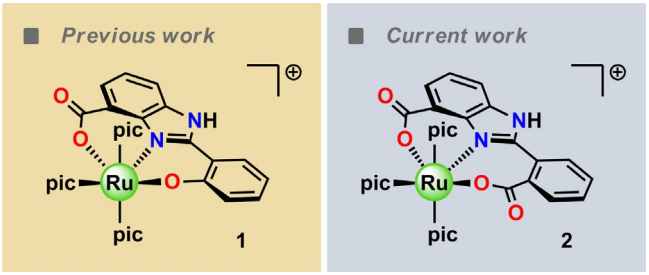

Figure 1. Molecular structures of single-site Ru complexes **1** and **2**.

In general, an ideal ligand scaffold should be able to bind strongly to the metal center(s), stabilize the metal in high oxidation states efficiently, and be resistant to oxidation. In this regard, negatively charged ligand frameworks are an appealing solution as they can stabilize the oxidized metal species formed within the water oxidation catalytic cycle.[10] Modification of the ligand framework can result in a dramatic change in reactivity, mechanism, and longevity of the developed

[a] Dr. A. F. Abdel-Magied, A. Shatskiy, T. M. Laine, Dr. W. A. A. Arafa, Prof. P. E. M. Siegbahn, Dr. M. D. Kärkäs, Prof. B. Åkermark, Dr. E. V. Johnston
Department of Organic Chemistry, Arrhenius Laboratory
Stockholm University
106 91 Stockholm (Sweden)
E-mail: markus.karkas@su.se
bjorn.akermark@su.se
eric.johnston@su.se

[b] Prof. R.-Z. Liao
Key Laboratory for Large-Format Battery Materials and System
Ministry of Education
School of Chemistry and Chemical Engineering
Huazhong University of Science and Technology
Wuhan 430074 (P.R. China)

[c] Dr. W. A. A. Arafa
Current address:
Chemistry Department, Faculty of Science
Fayoum University
PO Box 63514, Fayoum (Egypt)

Supporting Information and the ORCID identification number(s) for the author(s) of this article can be found under http://dx.doi.org/10.1002/cssc.201601171.

WOCs.[11] Recently, our group developed a single-site Ru-based catalyst **1** (Figure 1), which mediates chemical and photochemical water oxidation with high efficiency under neutral conditions both by pregenerated and photogenerated $[Ru(bpy)_3]^{3+}$.[12] The benzimidazole moiety embedded in the ligand structure was shown to act as a redox and proton transfer mediator, which leads to the increased activity of the catalyst. Inspired by these results, we were motivated to explore related benzimidazole-based Ru complexes for water oxidation. Herein we report the synthesis and characterization of single-site Ru complex **2**. The developed complex was found to catalyze water oxidation efficiently both chemically using $[Ru(bpy)_3]^{3+}$ and CAN as oxidants at pH 7.2 and 1.0, respectively, and photochemically assisted by a photosensitizer, $[Ru(bpy)_3]^{2+}$, and $Na_2S_2O_8$ as a sacrificial electron acceptor. Additionally, the generation of a formal high-valent Ru^{VI} species as a possible key intermediate during the catalytic oxidation of water was observed using ESI-HRMS. This work highlights the importance of the designed ligand framework to stabilize the metal center in high-valent oxidation states during the catalytic process.

Table 1. Redox potentials for complex **2** and related single-site Ru complexes.

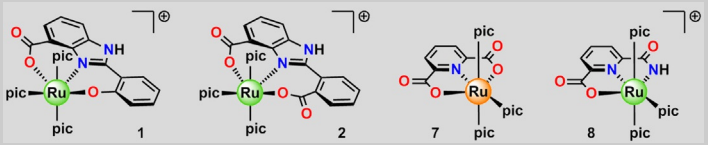

Entry	Complex	$E_{1/2}$ [V vs. NHE] Ru^{III}/Ru^{II}	Ru^{IV}/Ru^{III}	Ru^{V}/Ru^{IV}	Ru^{VI}/Ru^{V}	Ref.
1[a]	**1**	0.56	0.59	0.75	1.16	[12]
2[a]	**2**	0.06	0.51, 0.68	1.04	–	This work
3[b]	**7**	0.46	0.84	1.05	–	[10b]
4[a]	**8**	0.35	0.72	0.92	–	[10h]

[a] Electrochemical measurements were performed in an aqueous phosphate buffer solution (0.1 M, pH 7.2). All potentials were obtained from DPV and are reported vs. NHE. [b] Electrochemical measurements were performed in an aqueous phosphate buffer solution (0.05 M, pH 7.0) that contained 10% acetonitrile.

Results and Discussion

Synthesis and characterization

The ligand 2-(2-carboxyphenyl)-1*H*-benzo[*d*]imidazole-4-carboxylic acid (H_3cbc) and the related single-site Ru complex **2** were synthesized according to Scheme 1. The heating of a suspension of 2-carboxybenzaldehyde and 2-amino-3-nitrobenzoic acid in ethanol followed by the addition of a freshly prepared aqueous solution of $Na_2S_2O_4$ and the subsequent stirring of the reaction mixture at 70 °C for 5 h afforded H_3cbc as a pale yellow solid in 70% yield.

Ligand H_3cbc was heated to reflux with Et_3N and $[Ru(DMSO)_4Cl_2]$ in methanol under N_2 followed by the addition of an excess amount of 4-picoline with continued heating to afford the desired single-site Ru complex **2**, which was characterized fully by IR spectroscopy, ^{1}H NMR spectroscopy, elemental analysis, and ESI-HRMS. As a result of the paramagnetic shift exerted by the Ru^{III} d^5 ion in **2**, the ^{1}H NMR spectrum displayed broadened peaks. The Ru^{III} center was, therefore, reduced by the addition of 1.5 equivalents of ascorbic acid to give a diamagnetic Ru^{II} complex with sharp ^{1}H NMR peaks (Figure S3 in the Supporting Information). The ESI-HRMS signal at $m/z = 661.1109$ could be assigned to the molecular ion $[\mathbf{2}]^+$ and supports the structure of complex **2** (Figure S4).

The electrochemical properties of complex **2** were investigated using cyclic voltammetry (CV) and differential pulse voltammetry (DPV; Figures S5–S8). Under neutral conditions (0.1 M phosphate buffer, pH 7.2), the voltammograms displayed an intense electrocatalytic wave with an onset potential of approximately 1.04 V versus the normal hydrogen electrode (NHE), which was ascribed to electrocatalytic water oxidation (Figure S5). Furthermore, four peaks were observed in the DPV of **2** that were assigned to the Ru^{III}/Ru^{II} (0.06 V vs. NHE), Ru^{IV}/Ru^{III} (0.51 and 0.68 V vs. NHE), and Ru^{V}/Ru^{IV} (1.04 V vs. NHE) redox couples (based on comparison with the results from the DFT calculations). The redox potentials of complexes **1**, **2**, and some related mononuclear Ru complexes are shown in Table 1. The low redox potentials of complex **2** reflect the beneficial effect of the rational design of the dicarboxylate ligand.

Notably, the thermodynamic parameters derived from the electrochemical measurements are dependent on various factors, such as heterogeneous electron transfer kinetics, mass-transport regime, and coupled chemical reactions. Thus, the assigned values from different studies should be compared with caution.[13]

Catalytic water oxidation with chemical oxidants

The ability of complex **2** to catalyze water oxidation was evaluated using the sacrificial oxidants CAN and $[Ru(bpy)_3]^{3+}$ at pH 1.0 and 7.2, respectively. The mixing of the solution of the

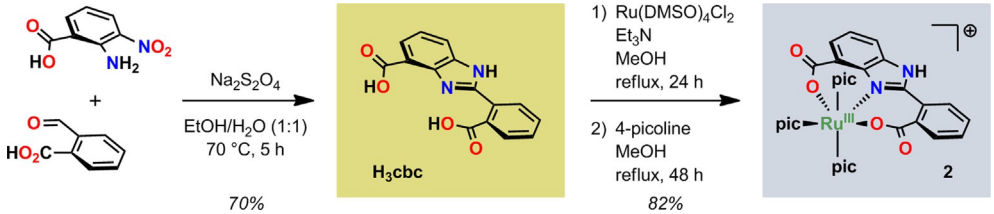

Scheme 1. Synthesis of H_3cbc and Ru complex **2** (pic = 4-picoline).

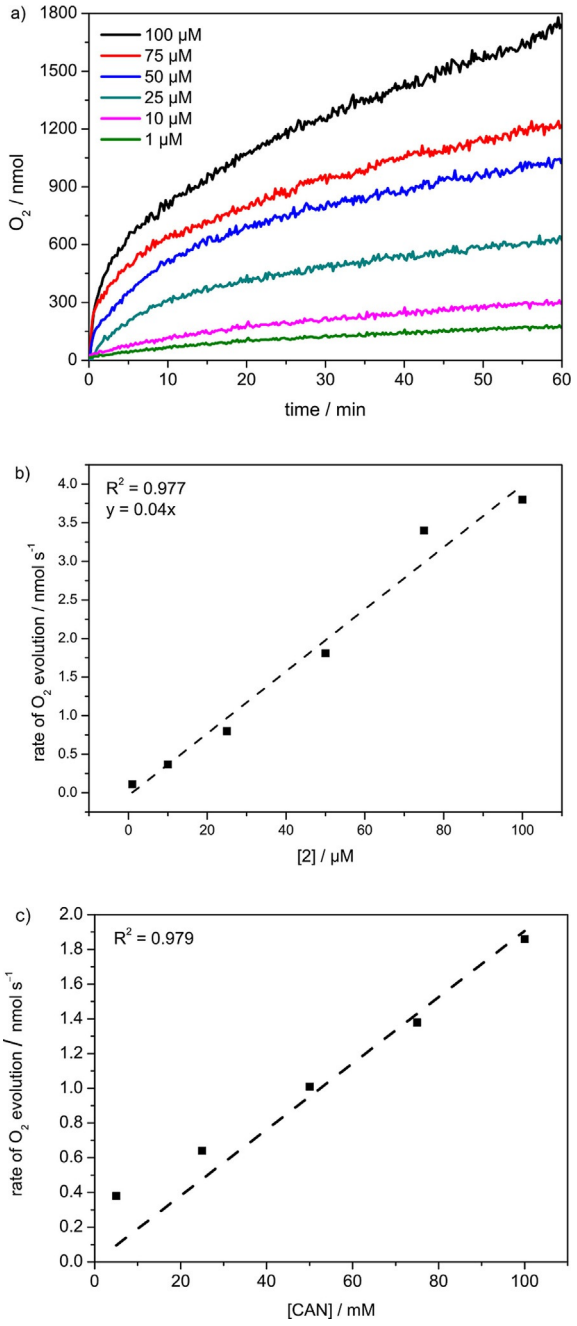

Figure 2. a) Plots of O_2 evolution versus time at various concentrations of Ru complex **2**. The catalytic experiments were performed by the addition of an aqueous CF_3CH_2OH/CF_3SO_3H (0.1 M, pH 1.0, 0.5 mL; v/v 2.5:97.5) solution that contained complex **2** in various concentrations to CAN (100 mM). b) Initial rates of O_2 evolution as a function of the concentrations of complex **2** (1.0–50 μM) at a fixed CAN concentration (100 mM). c) Plot of initial rate of O_2 evolution against CAN concentrations (5–100 mM) at a fixed concentration of complex **2** (50 μM).

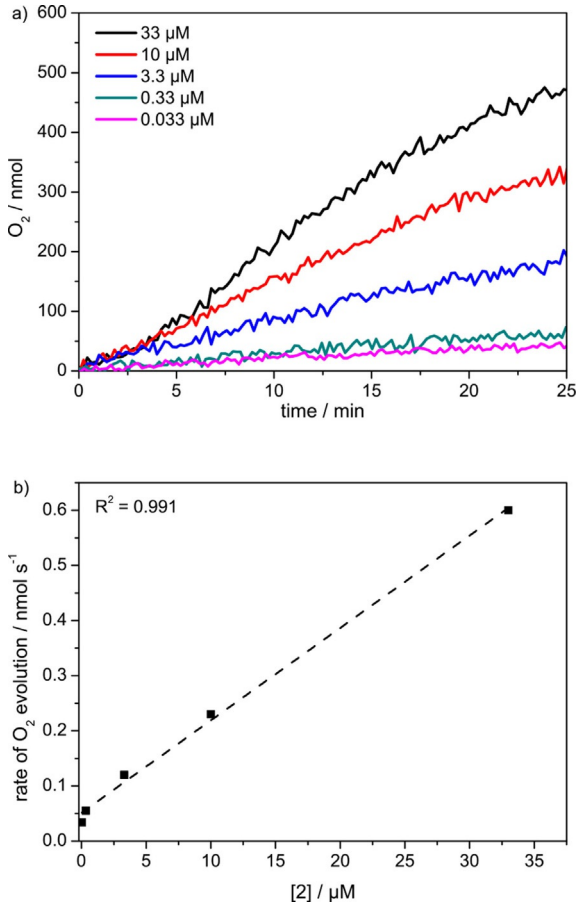

Figure 3. a) Plots of O_2 evolution versus time at various concentrations of Ru complex **2**. Reaction conditions: An aqueous phosphate buffer solution (0.1 M, pH 7.2, 0.5 mL) that contained complex **2** was added to $[Ru(bpy)_3](PF_6)_3$ (5.1 mg, 5.1 μmol). b) Initial rates of the O_2 evolution plotted as a function of the concentration of complex **2** (0.033–33 μM) at a fixed concentration of $[Ru(bpy)_3](PF_6)_3$ (5.1 μmol).

Table 2. Summary of the catalytic activity of Ru complex **2** in chemical water oxidation using CAN as the oxidant.[a]

Entry	[**2**] [μM]	[CAN] [mM]	O_2 [nmol]	TON[b]
1	100	100	1746	35
2	75	100	1230	33
3	50	100	1008	40
4	25	100	614	50
5	10	100	295	59
6	1	100	180	360
7	50	75	808	32
8	50	50	725	29
9	50	25	333	13
10	50	5	308	12

[a] Reaction conditions: An aqueous CF_3CH_2OH/CF_3SO_3H (0.1 M, pH 1.0; v/v 2.5:97.5, 0.50 mL) solution that contained the desired concentration of complex **2** was added to the appropriate amount of CAN, and the reaction was performed for 60 min. [b] TON = nmol O_2 per nmol catalyst.

catalyst and the solid oxidant resulted in an immediate O_2 evolution without any induction period and the amount of produced O_2 was monitored in the gas phase using real-time MS (Figures 2a and 3a). The initial rate of water oxidation with CAN as oxidant was pseudo-first order in **2**, which indicates that a single Ru site is involved in the rate-determining step of the catalytic cycle (Figure 2b; rate = $k_{obs} \times$ [**2**], in which k_{obs} is the pseudo-first-order rate constant). At a fixed concentration of **2** (50 μM), the oxidation was also pseudo-first order in CAN (Table 2, entries 3 and 7–10, Figure 2c). The turnover number

(TON) increased from 35 to 360 upon dilution of the complex from 100 to 1 μM. The initial turnover frequency (TOF = O_2 evolution rate/amount of **2** per second) of **2** can be calculated by converting the measured rate constant k_{obs} (0.04), which yields a moderate initial TOF of 0.08 s^{-1}.

To compare the catalytic performance of the single-site Ru catalyst **2** with that of **1**, $[Ru(bpy)_3]^{3+}$ was employed as oxidant and all measurements were conducted under similar catalytic conditions as those reported previously for complex **1**.[12] Complex **2** revealed an impressive catalytic activity for water oxidation, which resulted in a maximum TON of 3100 and an initial TOF of >2 s^{-1} (Figure 3a, Figure S9, and Table 3). A plot of the initial rates against catalyst concentration revealed a linear dependence, which indicates a pseudo-first-order kinetic behavior of **2** (Figure 3b). Notably, the oxygen evolution rate with $[Ru(bpy)_3]^{3+}$ is at least 25 times faster than that with Ce^{IV} as a terminal oxidant. The TONs reported for different Ru-based WOCs that utilize $[Ru(bpy)_3]^{3+}$ as an oxidant are given in Table 4.

Table 3. TONs and TOFs at different concentrations for Ru complex **2** using $[Ru(bpy)_3]^{3+}$ as the chemical oxidant.[a]

Entry	[**2**] [μM]	TON [mol_{O_2} mol_{cat}^{-1}]	TOF [mol_{O_2} mol_{cat}^{-1} s^{-1}]
1	33	31	0.02
2	10	78	0.04
3	3.3	218	0.11
4	0.33	575	0.33
5	0.033	3100	2.1

[a] Reaction conditions: An aqueous phosphate buffer solution (0.1 M, pH 7.2, 0.50 mL) that contained complex **2** was added to $[Ru(bpy)_3](PF_6)_3$ (5.1 mg, 5.1 μmol), and the reaction was performed for 25–40 min.

Table 4. Comparison of TONs for different Ru-based water oxidation catalysts using $[Ru(bpy)_3]^{3+}$ as chemical oxidant.

Catalyst	TON [mol_{O_2} mol_{cat}^{-1}]	Ref.
1	4000	Ref. [12]
2	3100	This work
8	280	Ref. [10h]
$[Ru(H_2pdca)(pic)_3]$[a]	400	Ref. [10i]
$[Ru(bda)(pic)_2]$[b]	30	Ref. [14]

[a] H_4pdca = 2,6-pyridine-dicarboxamide. [b] bda = 2,2′-bipyridine-6,6′-dicarboxylate. pic = 4-picoline.

Photochemical water oxidation using $[Ru(bpy)_3]^{2+}$-type photosensitizers

To evaluate the ability of the single-site Ru complex **2** to mediate light-driven water oxidation, a three-component system that consisted of a photosensitizer ($[Ru(bpy)_3]^{2+}$), $Na_2S_2O_8$ as a sacrificial electron acceptor, and **2** was employed under visible-light irradiation. At pH 7.2 and a catalyst concentration of 10 μM, a moderate TON of 40 was obtained. However, a decrease of the catalyst concentration to 0.33 μM resulted in a TON of 330 (at pH 7.2) and an even higher TON of 600 if the reaction was conducted at pH 6.0 (Figure 4). The higher maximum TON at a lower pH is most likely because of the higher stability of the oxidized photosensitizer under these conditions. The replacement of the mild photosensitizer $[Ru(bpy)_3]^{2+}$ with the stronger $[Ru(bpy)_2(deeb)]^{2+}$ photosensitizer ($E_{1/2}$ (Ru^{III}/Ru^{II}) = 1.40 V vs. NHE; deeb = diethyl(2,2′-bipyridine)-4,4′-dicarboxylate) did not improve the catalytic activity (Figure S10).

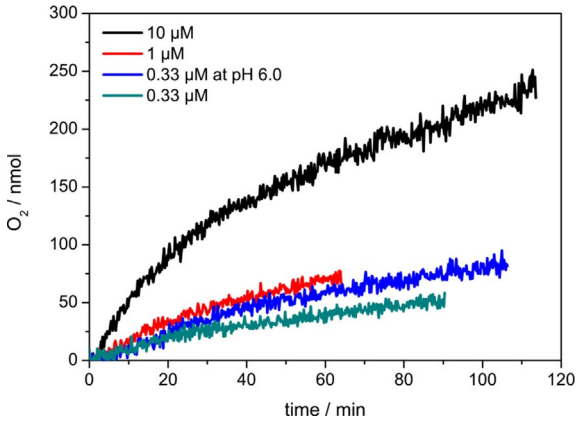

Figure 4. Light-driven water oxidation catalyzed by Ru complex **2**. Reaction conditions: An aqueous phosphate buffer solution (0.1 M, pH 7.2, or 6.0, 0.50 mL) that contained complex **2** was added to the photosensitizer $[Ru(bpy)_3](PF_6)_2$ (0.60 mM) and $Na_2S_2O_8$ (20 mM).

High-resolution mass spectrometry analysis

To enter the catalytic cycle, complex **2** has to undergo picoline (pic)–water ligand exchange, in which one of the picoline ligands is replaced by water to form a Ru-aqua species.[10,12] ESI-HRMS analysis of an aqueous solution of complex **2** revealed a peak at *m/z* 604.0282 (Figures 5a, b and 6), which corresponds to the diaqua species $[(Hcbc)Ru^{III}(OH_2)_2(pic)_2]^+$ (**3d** or **3e**; vide infra). This observation suggests that picoline–water exchange for Ru complex **2** could occur at the Ru^{III} state, which enables proton-coupled electron transfer (PCET) and easy access to higher redox states. Subsequently, ESI-HRMS was used to provide support for possible reaction intermediates that may form during water oxidation catalysis with **2**. Analysis of an aqueous solution of complex **2** that contained 15 equivalents of the oxidant $[Ru(bpy)_3]^{3+}$ revealed a signal at *m/z* 601.1095 in positive mode, which can be assigned to the high-valent Ru^{VI}-oxo species $[(Hcbc)Ru^{VI}(O)_2(pic)_2]+H^+$ ([**6d**/**6e** + H^+]$^+$), and the observed isotopic pattern is consistent with the proposed structure (Figures 5c and d, and 6).

Computational modeling and DFT calculations

To explain the redox behavior of **2**, DFT calculations were performed on the ligand-exchange reaction and the redox processes. At neutral pH, complex **2** in the Ru^{III} state was found to have a total charge of +1 (as the imidazole N atom is protonated), which is a doublet and the spin density on Ru is 0.83.

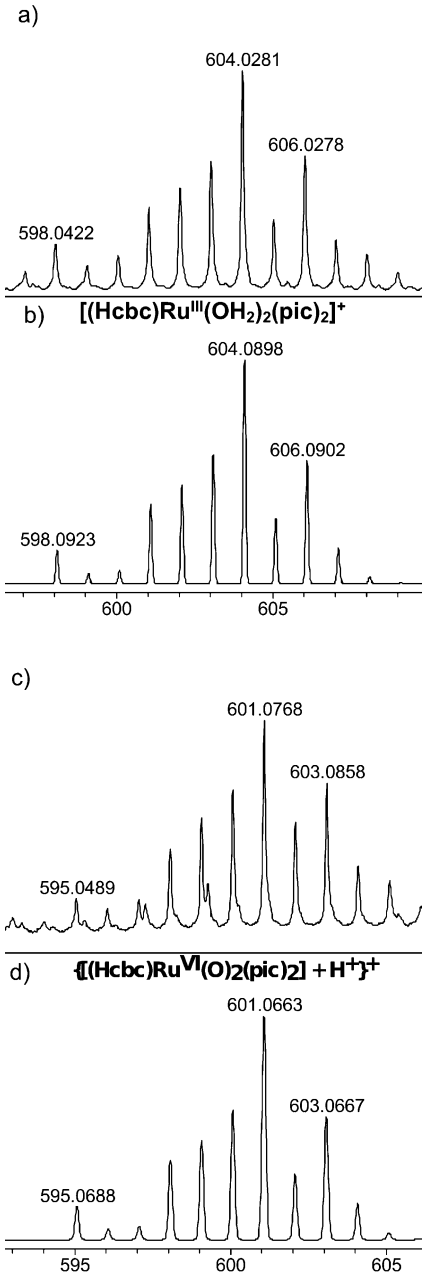

Figure 5. a) High-resolution mass spectrum of the $[(Hcbc)Ru^{III}(OH_2)_2(pic)_2]^+$ diaqua species ([**3d**/**3e**]$^+$) of complex **2** in positive mode, b) the simulated spectrum, c) high-resolution mass spectrum of $[(Hcbc)Ru^{VI}(O)_2(pic)_2+H^+]$ {[**6d**/**6e**$+H^+$]$^+$} in positive mode obtained after the addition of 15 equivalents of the oxidant $[Ru(bpy)_3](PF_6)_3$ to an aqueous solution of **2**, and d) the simulated spectrum.

The picoline-water ligand exchange for **2** at this oxidation state was investigated subsequently. Similar to that in complex **1**,[12] the equatorial picoline exchange to form aqua complex **3b** is slightly favored (endergonic by 10.4 kcal mol^{-1}) compared to the axial picoline exchange to form complex **3c** (endergonic by 14.0 kcal mol^{-1}; Figure 6). Our previous study revealed that the equatorial and axial picoline exchanges for **1** are endergonic by 11.7 and 14.2 kcal mol^{-1}, respectively. Therefore, the energy penalty for the ligand exchange for **2** is smaller than that of **1**, which suggests the faster formation of the Ru^{III}-aqua complex (**3b**). Both complexes **3b** and **3c** have a total charge of +1, and the energy of species **3c** was calculated to be +3.6 kcal mol^{-1} relative to **3b**. The pK_a of the aqua ligand in **3b** was calculated to be 8.9. Interestingly, the Ru-bound water molecule in complex **3c** forms a hydrogen bond to the carboxylate group with a distance of 1.68 Å. Next, the one-electron reduction potentials of complexes **2**, **3b**, and **3c** were calculated to be −0.08, −0.11, and −0.01 V, respectively. Under experimental conditions, complex **2** should be the dominant species in solution, and the calculated value of −0.08 V for the reduction of **2** agrees reasonably well with the experimental data (0.06 V; Table 5).

The oxidation of Ru^{III} complexes **3b** and **3c** to generate the Ru^{IV} complexes **4b** and **4c**, respectively, was then evaluated (Figure S13). It could be established that both oxidations were coupled with the release of two protons from the aqua ligand. The redox potentials were calculated to be 0.77 and 0.62 V, respectively, which is close to the two experimentally observed peaks (0.68 and 0.51 V). Therefore, these two peaks were assigned to the Ru^{IV}/Ru^{III} transitions that originate from two geometric isomers. Complexes **4b** and **4c** are both triplets and are close in energy, and the spin densities suggest that the formal Ru^{IV} complexes **4b** and **4c** are best described to feature a Ru^{III}-oxyl radical. The following oxidation of **4b** and **4c** had a different nature. The oxidation of **4b** to produce **5b** is suggested to be a PCET process (E = 1.12 V) as the pK_a of the protonated **5b** was calculated to be 6.8. However, the **4c**→**5c** transition is a one-electron oxidation process (E = 1.11 V) as the pK_a of complex **5c** was calculated to be 8.9. Importantly, the two calculated potentials are very close, which agrees with the fact that only a single peak at 1.04 V is observed experimentally. The subsequent one-electron oxidation of **5b** leads to the formal high-valent Ru^{VI} complex **6b**, which is a doublet and best formulated as a hybrid electronic structure of Ru^{VI}=O and Ru^{V}–O$^{\cdot}$. The redox potential for this transition was calculated to be

Table 5. Comparison of experimental and calculated redox potentials [V vs. NHE] for different intermediates derived from Ru complex **2**.

Experimental[a]		Calculated[b] a: $[Ru(pic)_3]^+$	b: $[Ru(pic)_2(OH_2)_{eq}]^+$	c: $[Ru(pic)_2(OH_2)_{ax}]^+$	d: $[Ru(pic)_2(OH_2)_2]$	e: $[Ru(pic)_2(OH_2)_2]$
Ru^{III}/Ru^{II}	0.06	−0.08	−0.11	−0.01	–	–
Ru^{IV}/Ru^{III}	0.51, 0.68	1.20	0.77	0.62	0.50	0.49
Ru^{V}/Ru^{IV}	1.04	–	1.12	1.11	0.89	1.08
Ru^{VI}/Ru^{V}	–	–	1.40	1.50	0.91	0.95

[a] Potentials were obtained using DPV in an aqueous phosphate buffer solution (0.1 M, pH 7.2). [b] Calculated at the B3LYP*-D2 level (for further details see Supporting Information). Species b and d correspond to equatorial picoline displaced by water, and c and e correspond to axial picoline displaced by water.

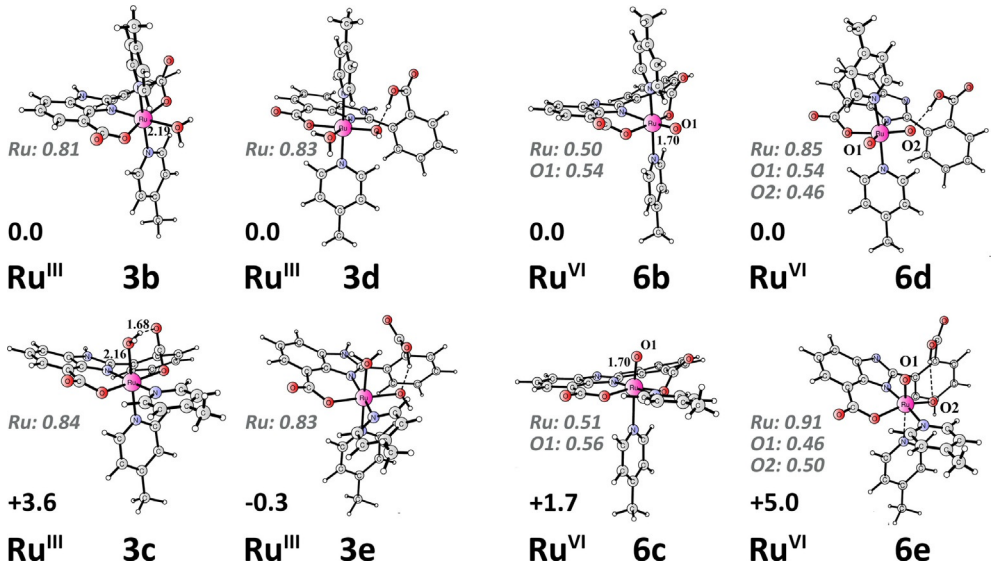

Figure 6. Optimized structures of selected Ru-aqua complexes and diaqua intermediates involved in water oxidation for Ru complex **2**. The formal oxidation states are highlighted, distances are given in Å, and spin densities for selected atoms are indicated in gray italic.

1.40 V. Instead, the oxidation of **5c** to **6c** is a PCET process associated with a potential of 1.50 V (for further details see the Supporting Information).

As species that correspond to the Ru^{III}-diaqua and Ru^{VI}-dioxo complexes were observed using ESI-HRMS, the insertion of an additional water molecule into the Ru-aqua complexes **3b** and **3c** at different redox states was also considered. During this process, the phenyl carboxylate unit dissociates from the Ru center to create an open site for the binding of the incoming water molecule. The addition of water at the Ru^{III} state for complex **3b** to generate **3d** is not favored as it was endergonic by 7.0 kcal mol^{-1} (Table S1). Water addition becomes more feasible at higher redox states as it is close to isogonic at the Ru^{IV} state and exergonic at the Ru^{V} and Ru^{VI} states. As complex **6b** has a total charge of +1, a proton is released into solution during the binding of the second water molecule, which was calculated to be exergonic by as much as 11.9 kcal mol^{-1} [Eq. (2)].

$$[(cbc)Ru^{VI}(O)(pic)_2]^+ \ (\mathbf{6b}) + H_2O \rightarrow [(Hcbc)Ru^{VI}(O)_2(pic)_2] \ (\mathbf{6d}) + H^+ \quad (2)$$
$$\Delta G = -11.9 \text{ kcal mol}^{-1}$$

The redox potentials for the oxidation of the Ru-diaqua complexes **3d** and **3e** are reported in Table 5, and the optimized structures are presented in Figure 6. The oxidations of **3d** and **3e** have very similar redox potentials of 0.495 and 0.494 V, respectively. These two values are lower than that of the oxidation of the corresponding monoaqua complexes **3b** and **3c**. At the Ru^{IV} state, water insertion becomes feasible; however, one may only observe the oxidation of the Ru^{IV}-aqua complex as the water addition is likely too slow to be observed on the timescale of the conducted electrochemical measurements. If it reaches the Ru^{V} state, the oxidation of the Ru^{V}-aqua complex is associated with quite a high redox potential (1.4 V). If water insertion becomes the dominant pathway, the oxidation of the Ru^{V}-diaqua complex can occur with a relatively low redox potential (0.912 and 0.947 V for complexes **5d** and **5e**, respectively; Figure S18).

Proposed catalytic pathway for O–O bond formation

Based on the obtained results, a catalytic cycle for water oxidation mediated by complex **2** was proposed (Scheme 2).[7n] The

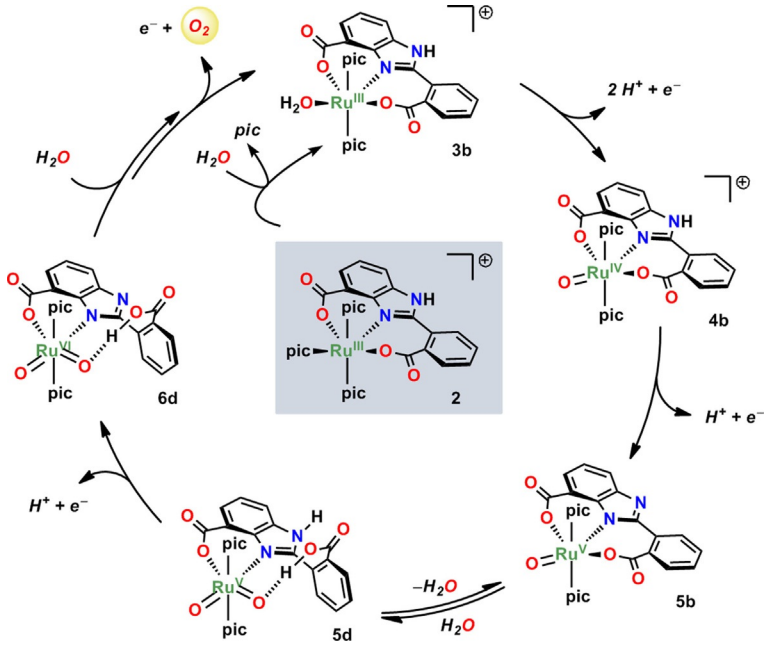

Scheme 2. Postulated mechanism for water oxidation by Ru complex **2**.

catalytic cycle is initiated by the formation of catalytically active Ru^{III}-aqua species **3** from complex **2** through ligand exchange of an equatorial picoline ligand by a water molecule. The Ru^{III}-aqua complex **3b** undergoes two PCET events to furnish the active Ru^{V} intermediate **5b**, which is presumed to be in equilibrium with the formal Ru^{V}-dioxo species **5d**. This high-valent Ru^{V} species can be further oxidized to the corresponding Ru^{VI}-dioxo complex **6d** (Figure 5c and d), which is believed to be responsible for mediating O–O bond formation in which an additional one-electron oxidation results in the release of O_2.

Conclusions

A single-site Ru^{III} complex **2** based on the negatively charged ligand cbc^{3-} has been developed. This study shows how rational ligand design can produce a water oxidation catalyst with a low onset potential, which allows water oxidation to be driven by the one-electron oxidants $[Ru(bpy)_3]^{3+}$ and $(NH_4)_2[Ce^{IV}(NO_3)_6]$. The catalytic activity of the developed complex **2** was comparable with that of the state-of-the-art Ru-based water oxidation catalysts using $[Ru(bpy)_3]^{3+}$ (TON up to 3100 with an initial turnover frequency (TOF) of $>2\ s^{-1}$ at pH 7.2), $(NH_4)_2[Ce^{IV}(NO_3)_6]$ (TON up to 316 with an initial TOF of $>0.08\ s^{-1}$ at pH 1.0), and $[Ru(bpy)_3]^{2+}$ (TON up to 600 with an initial TOF of $>0.03\ s^{-1}$ at pH 6.0) as the photosensitizer and $Na_2S_2O_8$ as the sacrificial electron acceptor in light-driven water oxidation. Experimental studies and DFT calculations support the interesting redox properties of complex **2** and reveal a peculiar operating mechanism that involves Ru-dioxo species stabilized by hydrogen bonding with the employed ligand. A detailed mechanistic study of the catalytic mechanism is in progress.

Experimental Section

All reactions and other manipulations were performed under nitrogen or argon atmosphere using standard Schlenk techniques. All reagents and solvents were obtained from commercial suppliers and used directly without further purification. The solvents were dried by standard techniques when needed. ^1H and ^{13}C NMR spectra were recorded using a Bruker UltraShield spectrometer at 500 or 400 and 101 MHz, respectively. Chemical shifts (δ) are reported in ppm using the residual solvent peak [[D_6]DMSO (δ(H) = 2.50 and (δ(C) = 39.52 ppm); $CDCl_3$ (δ(H) = 7.26)] as an internal standard. Splitting patterns are denoted as s (singlet), d (doublet), t (triplet), q (quartet), m (multiplet), dd (doublet of doublets), td (triplet of doublets), and br (broad). ESI-HRMS was performed using a Bruker Daltonics microTOF spectrometer. IR spectra were recorded using a PerkinElmer Spectrum One spectrometer using solid samples prepared as KBr discs. Elemental analysis was performed by MEDAC Ltd (Chobham, Surrey, UK). $[Ru(DMSO)_4Cl_2]$,[15] $[Ru(bpy)_3](PF_6)_3$,[16] $[Ru(bpy)_3](PF_6)_2$,[17] and $[Ru(bpy)_2(deeb)](PF_6)_2$[18] were synthesized according to literature methods.

Synthesis of 2-(2-carboxyphenyl)-1*H*-benzo[*d*]imidazole-4-carboxylic acid (H_3cbc)

A suspension of 2-carboxybenzaldehyde (1.00 g, 5.25 mmol) and 2-amino-3-nitrobenzoic acid (0.79 g, 1.57 mmol) in EtOH (30 mL) was prepared and stirred at room temperature for 20 min under N_2, followed by the addition of a solution of $Na_2S_2O_4$ (3.00 g, 17.24 mmol) in water (30 mL). The reaction mixture was stirred under N_2 at 70 °C for 5 h. The formed yellow precipitate was collected by filtration, washed with water (3×15 mL) and EtOH (3×15 mL), and dried under reduced pressure to afford the title compound as pale yellow solid (1.3 g, 70%). ^1H NMR (400 MHz, [D_6]DMSO): δ = 13.18 (bs, 3H), 7.92 (m, 3H), 7.84 (dd, J = 7.5, 1.5 Hz, 1H), 7.66 (td, J = 7.5, 1.5 Hz, 1H), 7.61 (td, J = 7.5, 1.5 Hz, 1H), 7.32 ppm (t, J = 7.8 Hz, 1H); ^{13}C NMR (101 MHz, [D_6]DMSO): δ = 169.3, 167.2, 153.8, 143.7, 135.4, 134.0, 131.5, 131.0, 130.4, 130.1, 130.0, 124.7, 123.4, 121.6, 115.8 ppm; IR (KBr disc): $\tilde{\nu}_{max}$ = 3069, 2920, 2521, 1707, 1627, 1575, 1548, 1461, 1375, 1350, 1279, 1185, 1119, 1008, 859, 764 cm^{-1}; ESI-HRMS (*m/z*): calcd for $C_{15}H_{10}N_2O_4$ $[M+H]^+$: 283.0719; found 283.1037.

Synthesis of complex 2

H_3cbc (150 mg, 0.51 mmol) and Et_3N (0.60 mL) were added to methanol (6.0 mL) and purged with N_2 for 10 min. $[Ru(DMSO)_4Cl_2]$ (258 mg, 0.51 mmol) was then added, and the reaction mixture was heated to reflux for 24 h under N_2. 4-Picoline (1.20 mL, 12.0 mmol) was added to the reaction mixture followed by further heating to reflux for 48 h. The dark-brown crude reaction mixture was concentrated to dryness and then redissolved in methanol (1.0 mL). The addition of water (2.0 mL) yielded a dark-green precipitate. The precipitate was isolated by filtration, washed with water (3×10 mL) and diethyl ether (3×10 mL), and dried under reduced pressure. The resulting product was purified by preparative TLC using glass plates coated with silica gel F_{254} (toluene/ethyl acetate mixture v/v 1:1 as eluent) to afford **2** as a dark-green solid (288 mg, 82%). ^1H NMR (500 MHz, $CDCl_3$): δ = 8.47 (d, J = 6.0 Hz, 1H), 8.43 (d, J = 6.6 Hz, 6H), 8.28 (d, J = 6.0 Hz, 2H), 8.10 (d, J = 7.9 Hz, 1H), 7.97 (d, J = 7.9 Hz, 1H), 7.47 (d, J = 7.9 Hz, 1H), 7.12 (d, J = 5.1 Hz, 1H), 6.90 (d, J = 6.4 Hz, 6H), 6.80 (d, J = 6.0 Hz, 1H), 2.63 (s, 3H), 2.35 ppm (s, 6H); IR (KBr disc): $\tilde{\nu}_{max}$ = 3433, 2977, 2938, 2604, 2496, 1618, 1495, 1443, 1397, 1127, 1036, 813, 1119, 764 cm^{-1}; ESI-HRMS (*m/z*): calcd for $C_{33}H_{29}N_5O_4Ru$ [**2**]$^+$: 661.1266; found 661.1109; elemental analysis (%) calcd for $C_{34}H_{33}ClN_5O_5RuS_{0.5}$ ([**2**]Cl·0.5 H_2O·0.5 DMSO): C 54.87, H 4.47, Cl 4.76, N 9.41; found: C 54.68, H 4.37, Cl 4.82, N 9.29.

Electrochemistry

Electrochemical measurements were performed using a potentiostat (CHI 750E, USA) interfaced to a personal computer and using a glassy carbon disk (diameter 3 mm) as the working electrode, a platinum wire as the counter electrode, and a saturated calomel electrode (SCE) as the reference electrode. The electrolyte used was an aqueous phosphate buffer solution (0.1 M, pH 7.2) or triflic acid (0.1 M, pH 1.0). All potentials are reported vs. NHE using the $[Ru(bpy)_3]^{3+}/[Ru(bpy)_3]^{2+}$ couple ($E_{1/2}$ = 1.26 V vs. NHE[19]) as a standard.

Chemical water oxidation

A stock solution of the Ru catalyst was made either in CF_3CH_2OH/CF_3SO_3H (v/v 2.5:97.5, 0.1 M CF_3SO_3H) or in phosphate buffer (0.1 M, pH 7.2) when CAN or $[Ru(bpy)_3](PF_6)_3$ was used as oxidants, respectively. The catalyst solutions used in the catalytic experiments were then prepared by diluting the stock solution to the desired concentration using either triflic acid (0.1 M, pH 1.0) or phosphate

buffer (0.1 M, pH 7.2). The resulting solutions were then purged with argon for at least 15 min before the catalytic experiments. Typically, the oxidant was placed in the reaction chamber and evacuated for at least 10 min. Subsequently, approximately 40 mbar He was introduced into the system followed by injection of the deoxygenated catalyst solution (0.50 mL). The evolved oxygen was then recorded over time using an MKS MicroVision Plus residual gas analyzer. See Ref. [2b] for a detailed description of the setup used.

Photochemical oxidation using $[Ru(bpy)_3]^{2+}$-type photosensitizers

The light source in these experiments was a halogen lamp. The reaction chamber was placed in a 100 mL glass vessel filled with water to avoid the heating of the system during catalysis and to filter out the UV light. The temperature was maintained at 16 °C using a circulating water-cooling system. Typically, the photosensitizer $[Ru(bpy)_3]^{2+}$ or $[Ru(bpy)_2(deeb)]^{2+}$ in acetonitrile (0.60 mM) and $Na_2S_2O_8$ (20 mM) were placed in the reaction chamber. The system was then evacuated with a rough pump to remove acetonitrile, and He was introduced into the system. After 15 min, the catalyst solution (0.50 mL) of the desired concentration was injected, and after an additional 5 min the light was switched on. The evolved oxygen was then recorded over time using an MKS MicroVision Plus residual gas analyzer.

Computational modeling and DFT calculations

The quantum chemical calculations were performed using the Gaussian 09 program package.[20] Geometries were optimized at the B3LYP[21]level using the effective core potential SDD[22] basis set for Ru and the 6-31G(d,p) basis set for the C, N, O, and H elements. Based on the optimized geometries, the final and the solvation energies in water were computed as a single-point using the SMD[23] continuum solvation model using the B3LYP* functional (15% exact exchange)[24] and a larger basis set, in which all elements, except Ru, were described by 6–311+G(2df,2p). Previously, it was shown that B3LYP* provides good redox potentials in photosystem II and some artificial water oxidation catalysts.[2h,7n,25] For the solvation free energy of water in water, the experimental value of $-6.3\ kcal\ mol^{-1}$ was used.[26] A concentration correction of 1.9 kcal mol^{-1} derived from the change of standard state in the gas phase (24.5 L mol^{-1} at 298.15 K) and in the water solution (1 mol L^{-1}) was added for all species except water, for which 4.3 kcal mol^{-1} was used inasmuch as the standard state of the water solvent is 55.6 M. Analytical frequency calculations were performed at the same level of theory as the geometry optimization to obtain the Gibbs free energy corrections. The B3LYP*-D2 free energies are reported, which include Gibbs free energy corrections from B3LYP and D2 dispersion corrections proposed by Grimme.[27] For the calculation of the redox potentials, exactly the same approach as in our previous study was adopted. Consequently, only some essential points are repeated here. The experimental absolute redox potential of the standard hydrogen electrode in water (4.281 V) was used as a reference,[28] which corresponds to an electron affinity of 98.72 kcal mol^{-1}. For the calculation of pK_a values, the experimental value of $-264.0\ kcal\ mol^{-1}$ for the solvation free energy of a proton is used,[26] and the total Gibbs free energy of a proton in water is $-270.3\ kcal\ mol^{-1}$.

Acknowledgements

Financial support from the Swedish Research Council (621-2013-4872), the Knut and Alice Wallenberg Foundation, and the Carl Trygger Foundation is gratefully acknowledged.

Keywords: electrochemistry · homogeneous catalysis · photochemistry · ruthenium · water oxidation

[1] M. Suga, F. Akita, K. Hirata, G. Ueno, H. Murakami, Y. Nakajima, T. Shimizu, K. Yamashita, M. Yamamoto, H. Ago, J.-R. Shen, *Nature* **2015**, *517*, 99–103.

[2] For recent examples of Mn-based water oxidation catalysts, see: a) M. Yagi, K. Narita, *J. Am. Chem. Soc.* **2004**, *126*, 8084–8085; b) Y. Gao, T. Åkermark, J. Liu, L. Sun, B. Åkermark, *J. Am. Chem. Soc.* **2009**, *131*, 8726–8727; c) M. M. Najafpour, T. Ehrenberg, M. Wiechen, P. Kurz, *Angew. Chem. Int. Ed.* **2010**, *49*, 2233–2237; *Angew. Chem.* **2010**, *122*, 2281–2285; d) R. K. Hocking, R. Brimblecombe, L.-Y. Chang, A. Singh, M. H. Cheah, C. Glover, W. H. Casey, L. Spiccia, *Nat. Commun.* **2011**, *3*, 461–466; e) E. A. Karlsson, B. L. Lee, T. Åkermark, E. V. Johnston, M. D. Kärkäs, J. Sun, Ö. Hansson, J. E. Bäckvall, B. Åkermark, *Angew. Chem. Int. Ed.* **2011**, *50*, 11715–11718; *Angew. Chem.* **2011**, *123*, 11919–11922; f) W. A. Arafa, M. D. Kärkäs, B. L. Lee, T. Åkermark, R.-Z. Liao, H. M. Berends, J. Messinger, P. E. Siegbahn, B. Åkermark, *Phys. Chem. Chem. Phys.* **2014**, *16*, 11950–11964; g) E. A. Karlsson, B.-L. Lee, R.-Z. Liao, T. Åkermark, M. D. Kärkäs, V. S. Becerril, P. E. M. Siegbahn, X. Zou, M. Abrahamsson, B. Åkermark, *ChemPlusChem* **2014**, *79*, 936–950; h) R.-Z. Liao, M. D. Kärkäs, B. L. Lee, B. Åkermark, P. E. M. Siegbahn, *Inorg. Chem.* **2015**, *54*, 342–351; i) L. Ma, Q. Wang, W.-L. Man, H.-K. Kwong, C.-C. Ko, T.-C. Lau, *Angew. Chem. Int. Ed.* **2015**, *54*, 5246–5249; *Angew. Chem.* **2015**, *127*, 5335–5338.

[3] For recent examples of Co-based water oxidation catalysts, see: a) Q. Yin, J. M. Tan, C. Besson, Y. V. Geletii, D. G. Musaev, A. E. Kuznetsov, Z. Luo, K. I. Hardcastle, C. L. Hill, *Science* **2010**, *328*, 342–345; b) D. K. Dogutan, R. McGuire, D. G. Nocera, *J. Am. Chem. Soc.* **2011**, *133*, 9178–9180; c) X. Zhou, F. Li, H. Li, B. Zhang, F. Yu, L. Sun, *ChemSusChem* **2014**, *7*, 2453–2456; d) H. Lv, J. Song, Y. V. Geletii, J. W. Vickers, J. M. Sumliner, D. G. Musaev, P. Kögerler, P. F. Zhuk, J. Bacsa, G. Zhu, C. L. Hill, *J. Am. Chem. Soc.* **2014**, *136*, 9268–9271; e) A. Han, H. Jia, H. Ma, S. Ye, H. Wu, H. Lei, Y. Han, R. Cao, P. Du, *Phys. Chem. Chem. Phys.* **2014**, *16*, 11224–11232; f) J. Liu, F. Du, H. Zhang, C. Lin, P. Gao, Y. Chen, Z. Shi, X. Li, T. Zhao, Y. Sun, *RSC Adv.* **2015**, *5*, 39075–39079.

[4] For recent examples of Fe-based water oxidation catalysts, see: a) J. L. Fillol, Z. Codolà, I. Garcia-Bosch, L. Gómez, J. J. Pla, M. Costas, *Nat. Commun.* **2011**, *3*, 807–813; b) C. Panda, J. Debgupta, D. Díaz Díaz, K. K. Singh, S. Sen Gupta, B. B. Dhar, *J. Am. Chem. Soc.* **2014**, *136*, 12273–12282; c) A. R. Parent, T. Nakazono, S. Lin, S. Utsunomiya, K. Sakai, *Dalton Trans.* **2014**, *43*, 12501–12513; d) B. M. Klepser, B. M. Bartlett, *J. Am. Chem. Soc.* **2014**, *136*, 1694–1697; e) F. Acuña-Parés, M. Costas, J. M. Luis, J. Lloret-Fillol, *Inorg. Chem.* **2014**, *53*, 5474–5485; f) M. K. Coggins, M.-T. Zhang, A. K. Vannucci, C. J. Dares, T. J. Meyer, *J. Am. Chem. Soc.* **2014**, *136*, 5531–5534; g) G. Panchbhai, W. M. Singh, B. Das, R. T. Jane, A. Thapper, *Eur. J. Inorg. Chem.* **2016**, 3262–3268; h) B. Das, A. Orthaber, S. Ott, A. Thapper, *ChemSusChem* **2016**, *9*, 1178–1186; i) B. Das, B.-L. Lee, E. A. Karlsson, T. Åkermark, A. Shatskiy, S. Demeshko, R.-Z. Liao, T. M. Laine, M. Haukka, E. Zeglio, A. F. Abdel-Magied, P. E. M. Siegbahn, F. Meyer, M. D. Kärkäs, E. V. Johnston, E. Nordlander, B. Åkermark, *Dalton Trans.* **2016**, *45*, 13289–13293.

[5] For recent examples of Cu-based water oxidation catalysts, see: a) S. M. Barnett, K. I. Goldberg, J. M. Mayer, *Nat. Commun.* **2012**, *4*, 498–502; b) M. K. Coggins, M.-T. Zhang, Z. Chen, N. Song, T. J. Meyer, *Angew. Chem. Int. Ed.* **2014**, *53*, 12226–12230; *Angew. Chem.* **2014**, *126*, 12422–12426; c) P. Garrido-Barros, I. Funes-Ardoiz, S. Drouet, J. Benet-Buchholz, F. Maseras, A. Llobet, *J. Am. Chem. Soc.* **2015**, *137*, 6758–6761; d) X.-J. Su, M. Gao, L. Jiao, R.-Z. Liao, P. E. M. Siegbahn, J.-P. Cheng, M.-T. Zhang, *Angew. Chem. Int. Ed.* **2015**, *54*, 4909–4914; *Angew. Chem.* **2015**, *127*, 4991–4996; e) R.-J. Xiang, H.-Y. Wang, Z.-J. Xin, C.-B. Li, Y.-X. Lu, X.-W. Gao, H.-M. Sun, R. Cao, *Chem. Eur. J.* **2016**, *22*, 1602–1607.

[6] For recent examples of Ir-based water oxidation catalysts, see a) N. D. McDaniel, F. J. Coughlin, L. L. Tinker, S. Bernhard, *J. Am. Chem. Soc.* **2008**, *130*, 210 – 217; b) J. F. Hull, D. Balcells, J. D. Blakemore, C. D. Incarvito, O. Eisenstein, G. W. Brudvig, R. H. Crabtree, *J. Am. Chem. Soc.* **2009**, *131*, 8730 – 8731; c) R. Lalrempuia, N. D. McDaniel, H. Müller-Bunz, S. Bernhard, M. Albrecht, *Angew. Chem. Int. Ed.* **2010**, *49*, 9765 – 9768; *Angew. Chem.* **2010**, *122*, 9959 – 9962; d) M. Navarro, M. Li, H. Müller-Bunz, S. Bernhard, M. Albrecht, *Chem. Eur. J.* **2016**, *22*, 6740 – 6745; e) A. Bucci, G. M. Rodriguez, G. Bellachioma, C. Zuccaccia, A. Poater, L. Cavallo, A. Macchioni, *ACS Catal.* **2016**, *6*, 4559 – 4563.

[7] For recent examples of Ru-based water oxidation catalysts, see: a) Y. Xu, T. Åkermark, V. Gyollai, D. Zou, L. Eriksson, L. Duan, R. Zhang, B. Åkermark, L. Sun, *Inorg. Chem.* **2009**, *48*, 2717 – 2719; b) Y. Xu, L. Duan, L. Tong, B. Åkermark, L. Sun, *Chem. Commun.* **2010**, *46*, 6506 – 6508; c) Y. Xu, A. Fischer, L. Duan, L. Tong, E. Gabrielsson, B. Åkermark, L. Sun, *Angew. Chem. Int. Ed.* **2010**, *49*, 8934 – 8937; *Angew. Chem.* **2010**, *122*, 9118 – 9121; d) M. D. Kärkäs, E. V. Johnston, E. A. Karlsson, B. L. Lee, T. Åkermark, M. Shariatgorji, L. Ilag, Ö. Hansson, J. E. Bäckvall, B. Åkermark, *Chem. Eur. J.* **2011**, *17*, 7953 – 7959; e) Y. Xu, L. Duan, T. Åkermark, L. Tong, B. L. Lee, R. Zhang, B. Åkermark, L. Sun, *Chem. Eur. J.* **2011**, *17*, 9520 – 9528; f) L. Wang, L. Duan, B. Stewart, M. Pu, J. Liu, T. Privalov, L. Sun, *J. Am. Chem. Soc.* **2012**, *134*, 18868 – 18880; g) M. D. Kärkäs, T. Åkermark, H. Chen, J. Sun, B. Åkermark, *Angew. Chem. Int. Ed.* **2013**, *52*, 4189 – 4193; *Angew. Chem.* **2013**, *125*, 4283 – 4287; h) Y. Liu, S.-M. Ng, S.-M. Yiu, W. W. Y. Lam, X.-G. Wei, K. C. Lau, *Angew. Chem. Int. Ed.* **2014**, *53*, 14468 – 14471; *Angew. Chem.* **2014**, *126*, 14696 – 14699; i) J. T. Muckerman, M. Kowalczyk, Y. M. Badiei, D. E. Polyansky, J. J. Concepcion, R. Zong, R. P. Thummel, E. Fujita, *Inorg. Chem.* **2014**, *53*, 6904 – 6913; j) Y. Wang, M. S. G. Ahlquist, *Phys. Chem. Chem. Phys.* **2014**, *16*, 11182 – 11185; k) A. C. Sander, S. Maji, L. Francas, T. Böhnisch, S. Dechert, A. Llobet, F. Meyer, *ChemSusChem* **2015**, *8*, 1697 – 1702; l) T. M. Laine, M. D. Kärkäs, R.-Z. Liao, P. E. M. Siegbahn, B. Åkermark, *Chem. Eur. J.* **2015**, *21*, 10039 – 10048; m) L. Tong, R. Zong, R. Zhou, N. Kaveevivitchai, G. Zhang, R. Thummel, *Faraday Discuss.* **2015**, *185*, 87 – 104; n) M. D. Kärkäs, R.-Z. Liao, T. M. Laine, T. Åkermark, S. Ghanem, P. E. M. Siegbahn, B. Åkermark, *Catal. Sci. Technol.* **2016**, *6*, 1306 – 1319; o) M. Schulze, V. Kunz, P. D. Frischmann, F. Würthner, *Nat. Chem.* **2016**, *8*, 576 – 583.

[8] J. Limburg, J. S. Vrettos, L. M. Liable-Sands, A. L. Rheingold, R. H. Crabtree, G. W. Brudvig, *Science* **1999**, *283*, 1524 – 1527.

[9] J. Limburg, J. S. Vrettos, H. Chen, J. C. de Paula, R. H. Crabtree, G. W. Brudvig, *J. Am. Chem. Soc.* **2001**, *123*, 423 – 430.

[10] a) L. Duan, A. Fischer, Y. Xu, L. Sun, *J. Am. Chem. Soc.* **2009**, *131*, 10397 – 10399; b) L. Duan, Y. Xu, M. Gorlov, L. Tong, S. Andersson, L. Sun, *Chem. Eur. J.* **2010**, *16*, 4659 – 4668; c) L. Duan, F. Bozoglian, S. Mandal, B. Stewart, T. Privalov, A. Llobet, L. Sun, *Nat. Chem.* **2012**, *4*, 418 – 423; d) L. Tong, Y. Wang, L. Duan, Y. Xu, X. Cheng, A. Fischer, M. S. G. Ahlquist, L. Sun, *Inorg. Chem.* **2012**, *51*, 3388 – 3398; e) Y. Jiang, F. Li, B. Zhang, X. Li, X. Wang, F. Huang, L. Sun, *Angew. Chem. Int. Ed.* **2013**, *52*, 3398 – 3401; *Angew. Chem.* **2013**, *125*, 3482 – 3485; f) L. Duan, L. Wang, A. K. Inge, A. Fischer, X. Zou, L. Sun, *Inorg. Chem.* **2013**, *52*, 7844 – 7852; g) T. M. Laine, M. D. Kärkäs, R.-Z. Liao, T. Åkermark, B.-L. Lee, E. A. Karlsson, P. E. M. Siegbahn, B. Åkermark, *Chem. Commun.* **2015**, *51*, 1862 – 1865; h) W. Rabten, M. D. Kärkäs, T. Åkermark, H. Chen, R.-Z. Liao, F. Tinnis, J. Sun, P. E. M. Siegbahn, P. G. Andersson, B. Åkermark, *Inorg. Chem.* **2015**, *54*, 4611 – 4620; i) W. Rabten, T. Åkermark, M. D. Kärkäs, H. Chen, J. Sun, P. G. Andersson, B. Åkermark, *Dalton Trans.* **2016**, *45*, 3272 – 3276; j) R.-Z. Liao, M. D. Kärkäs, T. M. Laine, B. Åkermark, P. E. M. Siegbahn, *Catal. Sci. Technol.* **2016**, *6*, 5031 – 5041.

[11] For recent reviews on water oxidation catalysts, see: a) M. D. Kärkäs, O. Verho, E. V. Johnston, B. Åkermark, *Chem. Rev.* **2014**, *114*, 11863 – 12001; b) J. D. Blakemore, R. H. Crabtree, G. W. Brudvig, *Chem. Rev.* **2015**, *115*, 12974 – 13005; c) M. Okamura, S. Masaoka, *Chem. Asian J.* **2015**, *10*, 306 – 315; d) L. Duan, L. Wang, F. Li, F. Li, L. Sun, *Acc. Chem. Res.* **2015**, *48*, 2084 – 2096; e) M. D. Kärkäs, B. Åkermark, *Dalton Trans.* **2016**, *45*, 14421 – 14461; f) L. Tong, R. P. Thummel, *Chem. Sci.* **2016**, *7*, 6591 – 6603.

[12] M. D. Kärkäs, T. Åkermark, E. V. Johnston, S. R. Karim, T. M. Laine, B. L. Lee, T. Åkermark, T. Privalov, B. Åkermark, *Angew. Chem. Int. Ed.* **2012**, *51*, 11589 – 11593; *Angew. Chem.* **2012**, *124*, 11757 – 11761.

[13] E. S. Rountree, B. D. McCarthy, T. T. Eisenhart, J. L. Dempsey, *Inorg. Chem.* **2014**, *53*, 9983 – 10002.

[14] L. Duan, Y. Xu, P. Zhang, M. Wang, L. Sun, *Inorg. Chem.* **2010**, *49*, 209 – 215.

[15] E. Dulière, M. Devillers, J. Marchand-Brynaert, *Organometallics* **2003**, *22*, 804 – 811.

[16] R. E. DeSimone, R. S. Drago, *J. Am. Chem. Soc.* **1970**, *92*, 2343 – 2352.

[17] M. M. Taqui Khan, R. C. Bhardwaj, C. Bhardwaj, *Polyhedron* **1990**, *9*, 1243 – 1248.

[18] a) B. P. Sullivan, D. J. Salmon, T. J. Meyer, *Inorg. Chem.* **1978**, *17*, 3334 – 3341; b) A. R. Oki, R. J. Morgan, *Synth. Commun.* **1995**, *25*, 4093 – 4097; c) H. Xia, Y. Zhu, D. Lu, M. Li, C. Zhang, B. Yang, Y. Ma, *J. Phys. Chem. B* **2006**, *110*, 18718 – 18723.

[19] A. Juris, V. Balzani, F. Barigelletti, S. Campagna, P. Belser, A. von Zelewsky, *Coord. Chem. Rev.* **1988**, *84*, 85 – 277.

[20] Gaussian 09, Revision D.01, M. J. Frisch, G. W. Trucks, H. B. Schlegel, G. E. Scuseria, M. A. Robb, J. R. Cheeseman, G. Scalmani, V. Barone, B. Mennucci, G. A. Petersson, H. Nakatsuji, M. Caricato, X. Li, H. P. Hratchian, A. F. Izmaylov, J. Bloino, G. Zheng, J. L. Sonnenberg, M. Hada, M. Ehara, K. Toyota, R. Fukuda, J. Hasegawa, M. Ishida, T. Nakajima, Y. Honda, O. Kitao, H. Nakai, T. Vreven, J. A. Montgomery Jr., J. E. Peralta, F. Ogliaro, M. Bearpark, J. J. Heyd, E. Brothers, K. N. Kudin, V. N. Staroverov, R. Kobayashi, J. Normand, K. Raghavachari, A. Rendell, J. C. Burant, S. S. Iyengar, J. Tomasi, M. Cossi, N. Rega, M. J. Millam, M. Klene, J. E. Knox, J. B. Cross, V. Bakken, C. Adamo, J. Jaramillo, R. Gomperts, R. E. Stratmann, O. Yazyev, A. J. Austin, R. Cammi, C. Pomelli, J. W. Ochterski, R. L. Martin, K. Morokuma, V. G. Zakrzewski, G. A. Voth, P. Salvador, J. J. Dannenberg, S. Dapprich, A. D. Daniels, Ö. Farkas, J. B. Foresman, J. V. Ortiz, J. Cioslowski, D. J. Fox, Gaussian, Inc., Wallingford CT, **2009**.

[21] A. D. Becke, *J. Chem. Phys.* **1993**, *98*, 5648 – 5652.

[22] D. Andrae, U. Häußermann, M. Dolg, H. Stoll, H. Preuß, *Theor. Chim. Acta.* **1990**, *77*, 123 – 141.

[23] A. V. Marenich, C. J. Cramer, D. G. Truhlar, *J. Phys. Chem. B* **2009**, *113*, 6378 – 6396.

[24] M. Reiher, O. Salomon, B. A. Hess, *Theor. Chem. Acc.* **2001**, *107*, 48 – 55.

[25] a) X. Li, G. Chen, S. Schinzel, P. E. M. Siegbahn, *Dalton Trans.* **2011**, *40*, 11296 – 11307; b) P. E. M. Siegbahn, M. R. A. Blomberg, *J. Chem. Theory Comput.* **2014**, *10*, 268 – 272; c) R.-Z. Liao, X. Li, P. E. M. Siegbahn, *Eur. J. Inorg. Chem.* **2014**, 728 – 741; d) R.-Z. Liao, P. E. M. Siegbahn, *ACS Catal.* **2014**, *4*, 3937 – 3949.

[26] D. M. Camaioni, C. A. Schwerdtfeger, *J. Phys. Chem. A* **2005**, *109*, 10795 – 10797.

[27] S. Grimme, *J. Comput. Chem.* **2006**, *27*, 1787 – 1799.

[28] A. A. Isse, A. Gennaro, *J. Phys. Chem. B* **2010**, *114*, 7894 – 7899.

Manuscript received: August 23, 2016
Final Article published: December 14, 2016

